

True hero of the trade: On the critical contributions of Art Gossard to modern device technology

Cite as: J. Vac. Sci. Technol. A **39**, 020804 (2021); <https://doi.org/10.1116/6.0000792>

Submitted: 17 November 2020 . Accepted: 14 January 2021 . Published Online: 18 February 2021

 Aaron J. Muhowski, Alec M. Skipper, Stephen D. March, Mark J. W. Rodwell, and Seth R. Bank

COLLECTIONS

Paper published as part of the special topic on [Honoring Dr. Art Gossard's 85th Birthday and His Leadership in the Science and Technology of Molecular Beam Epitaxy](#)



View Online



Export Citation



CrossMark

ARTICLES YOU MAY BE INTERESTED IN

[Quantum dot lasers—History and future prospects](#)

Journal of Vacuum Science & Technology A **39**, 020802 (2021); <https://doi.org/10.1116/6.0000768>

[Band parameters for III-V compound semiconductors and their alloys](#)

Journal of Applied Physics **89**, 5815 (2001); <https://doi.org/10.1063/1.1368156>

[Review of key vertical-cavity laser and modulator advances enabled by advanced MBE technology](#)

Journal of Vacuum Science & Technology A **39**, 010801 (2021); <https://doi.org/10.1116/6.0000574>

HIDEN
ANALYTICAL

Instruments for Advanced Science

- Knowledge,
- Experience,
- Expertise

[Click to view our product catalogue](#)

Contact Hiden Analytical for further details:

www.HidenAnalytical.com
info@hiden.co.uk



Gas Analysis

- ▶ dynamic measurement of reaction gas streams
- ▶ catalysis and thermal analysis
- ▶ molecular beam studies
- ▶ dissolved species probes
- ▶ fermentation, environmental and ecological studies



Surface Science

- ▶ UHVTPD
- ▶ SIMS
- ▶ end point detection in ion beam etch
- ▶ elemental imaging - surface mapping



Plasma Diagnostics

- ▶ plasma source characterization
- ▶ etch and deposition process reaction kinetic studies
- ▶ analysis of neutral and radical species



Vacuum Analysis

- ▶ partial pressure measurement and control of process gases
- ▶ reactive sputter process control
- ▶ vacuum diagnostics
- ▶ vacuum coating process monitoring

True hero of the trade: On the critical contributions of Art Gossard to modern device technology

Cite as: J. Vac. Sci. Technol. A 39, 020804 (2021); doi: 10.1116/6.0000792

Submitted: 17 November 2020 · Accepted: 14 January 2021 ·

Published Online: 18 February 2021




View Online



Export Citation



CrossMark

Aaron J. Muhowski,¹  Alec M. Skipper,¹ Stephen D. March,¹ Mark J. W. Rodwell,² and Seth R. Bank^{1,a)}

AFFILIATIONS

¹Department of Electrical and Computer Engineering, University of Texas Austin, Austin, Texas 78758

²Department of Electrical and Computer Engineering, University of California at Santa Barbara, Santa Barbara, California 93106

Note: This paper is part of the Special Topic Collection: Honoring Dr. Art Gossard's 85th Birthday and his Leadership in the Science and Technology of Molecular Beam Epitaxy.

^{a)}Electronic mail: sbank@utexas.edu

ABSTRACT

Professor Arthur Gossard's seminal contributions to fundamental physics often overshadow the immense impact he has had on advancing the performance and functionality of electronic and photonic devices. This paper attempts to, at least in part, capture this important aspect of Gossard's continuing research contributions by reviewing three disparate examples, along with their device applications: epitaxial regrowth, digital alloy growth, and metal:semiconductor nanocomposites.

Published under license by AVS. <https://doi.org/10.1116/6.0000792>

I. INTRODUCTION

As part of this Special Issue honoring Professor Arthur Gossard's continuing scientific and technological contributions, our goal here is to examine several areas in which he has profoundly expanded the materials portfolio and synthesis capabilities available to device designers, *as well as* advanced the performance and functionality of electronic and photonic devices. As will hopefully be evident from the following discussion, Art is one of those rare physicists and material scientists who seems to draw as much enjoyment from driving technological capabilities as he does advancing fundamental science. Consistent with this, a unique hallmark of his research is that he is as adept at inventing new materials approaches to solve current device limitations as he is at identifying clever device applications to leverage new materials innovations. His eminently collaborative approach to research coupled with his impressive ability to distill complex problems down to their essence and explain them clearly has led to a litany of incredibly successful collaborations with device designers and physicists over the years.

His embrace of collaboration was evident throughout his years at Bell Labs and has only deepened at University of California,

Santa Barbara (UCSB). He set the tone for the culture of the UCSB molecular beam epitaxy (MBE) lab; rather than siloes of MBE systems and researchers in isolated labs, he built and has continuously directed an open-access MBE facility where near countless faculty, postdocs, and students not only share resources, but openly share ideas. Those who have been fortunate enough to be involved with the UCSB MBE lab (e.g., MJWR and SRB) are forever changed by its unique atmosphere—one that values high-risk/high-reward collaborative research and open exchange of information. This has led to significant cross-pollination of new ideas across different domains over the years, some of which we hope to capture in this Review. If Herb Kroemer is the cornerstone upon which III-V semiconductor research at UCSB was built, Art has been its linchpin.

Any attempt to review all of Art's contributions to modern electronic and photonic devices would simply prove intractable. Therefore, we focus here on a subset of crucial fundamental materials technologies that he pioneered or helped pioneer: epitaxial regrowth (Sec. II), digital alloy growth (Sec. III), and metal:semiconductor nanocomposites (Sec. IV). In each case, we attempt to capture both their impact on current electronic and photonic

devices, as well as conclude (Sec. V) with an outlook on future opportunities.

II. EPITAXIAL REGROWTH

Art Gossard's strength as a materials scientist comes not only from his ability to develop novel growth techniques, but also from his commitment to taking his work from material studies to produce practical devices. Gossard's work on MBE regrowth for high-speed electronics is an outstanding example of this. While epitaxial regrowth, the process of performing additional crystal growth steps on already grown and fabricated material, was widely used in InGaAsP buried heterojunction lasers,¹⁻⁵ MBE regrowth was widely considered impractical due to the challenges of achieving selective area growth. Gossard with Rodwell and others were able to cleverly overcome this challenge by first designing devices that do not require selective area growth, and later advancing the material quality of MBE-regrown devices using periodic growth interruptions. This work predated further advances in MBE regrowth for photonic crystal surface emitting lasers,⁶ III-V on silicon metamorphics,⁷ and embedded dielectric structures⁸ once again demonstrating Gossard's ability to recognize the potential of unconventional materials science approaches to devices.

Gossard and Rodwell first utilized nonselective MBE to address the challenges of creating low-resistance contacts for double heterojunction bipolar transistors (DHBTs). Drawing inspiration from SiGe technology, nonselective regrowth was used to create wide area, highly doped, extrinsic emitter contacts to reduce the emitter resistance of the DHBT.⁹ While MBE was not conventionally used for regrown structures due to the fact that typical growth conditions result in polycrystalline deposition on metal and dielectric regions of a device structure, this allowed for the creation of an emitter contact larger than the base-emitter junction, thereby reducing the contact resistance compared to a conventional DHBT. By leveraging this apparent "weakness" of MBE regrowth, record RF

results were achieved for III-V regrown emitter heterojunction bipolar transistors (HBTs),^{9,10} demonstrating the potential of this growth technique (Fig. 1). In order to expand this process to MOSFET source and drain regions, MBE regrowth needed to be optimized to result in smooth, conformal films. III-V MOSFETs require low contact resistance and high source and drain doping to achieve high drive currents. Since ion implantation is impractical for achieving high doping in InGaAs and the channel must have high carrier mobility, doped regrowth is ideal for the source and drain regions of an InGaAs channel MOSFET. Due to the nonselective nature of MBE regrowth, a height dependent etch was developed to prevent regrowth from short-circuiting the source, drain, and gate.¹¹ This allowed for the fabrication of regrown source/drain MOSFETs; however, the initial devices were limited by high source resistance caused by a gap in the regrowth near the gate.¹² Wistey *et al.* implemented migration enhanced epitaxy (MEE) in order to produce smooth, highly-doped films without gaps.¹³ While conventional MBE growth supplies a constant flux of group III and group V atoms, MEE alternates between supplying the group III and group V species thereby increasing adatom mobility on the growth surface. This resulted in an order-of-magnitude improvement in both drive current and transconductance in the regrown MOSFETs.¹⁴ Furthermore, optimizing these devices resulted in a significant progress toward understanding the growth dynamics of MBE regrowth. Wistey *et al.* reported that a metal modulation epitaxy (MME) technique resulted in smoother conformal films.¹⁵ MME periodically interrupts the supply group III species similar to MEE, but supplies a constant group V flux instead of cycling it as well. While higher arsenic fluxes resulted in faceting of the growth front, reducing the arsenic flux yielded the desired film coverage and improved material quality. This improved understanding of MBE growth kinetics allowed for the advancement of Gossard and Rodwell's electronic devices and paved the way for future innovations in MBE regrowth (Fig. 2).

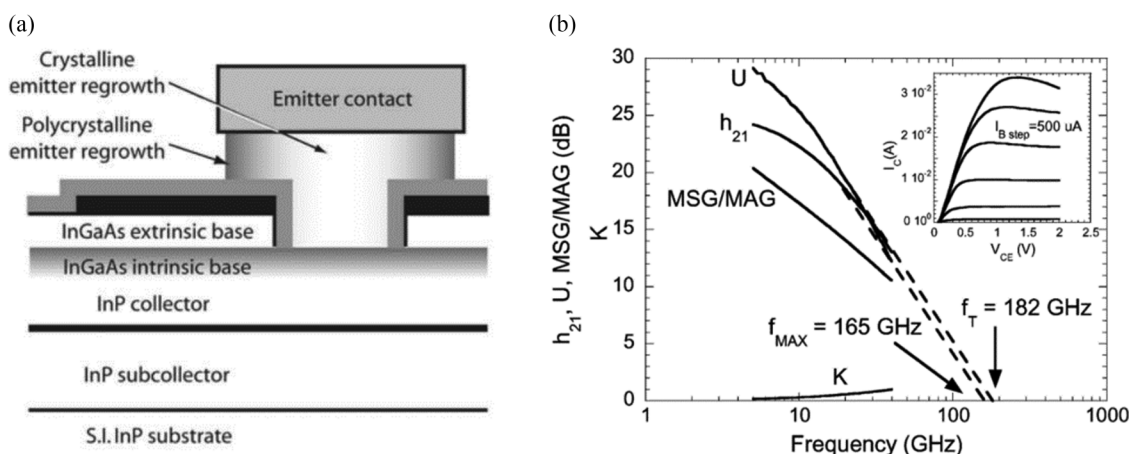


FIG. 1. (a) Diagram of a DHBT using a regrown n-doped InP and InGaAs emitter. (b) RF gain and stability curve for the $0.7 \times 8 \mu\text{m}^2$ InP-based regrown-emitter transistor shown in (a) with an inset common-emitter IV curve. Reprinted with permission from Scott *et al.*, IEEE Electron Device Lett. 25(6), 360 (2004). Copyright 2004, IEEE.

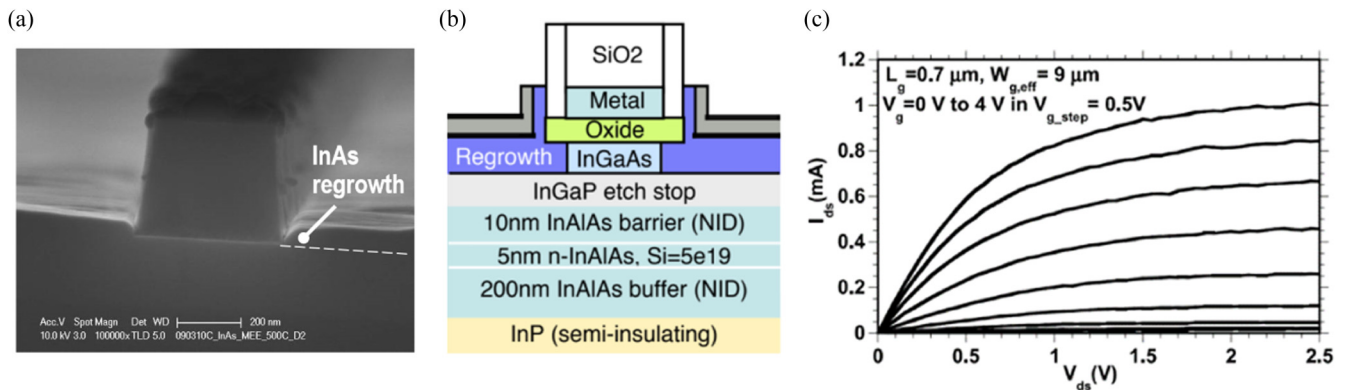


FIG. 2. (a) Cross-sectional scanning electron microscope image of a regrown source and drain using MEE. Reprinted with permission from Singiseti *et al.*, *IEEE Electron Device Lett.* **30**, 1128 (2009). Copyright 2009, IEEE. (b) Diagram of an MOSFET using source and drain regrowth by MEE. Figure courtesy of Mark Wistey (Ref. 13). (c) IV curve of an MOSFET using source and drain regrowth by MEE. Reprinted with permission from Singiseti *et al.*, in *IEEE International Conference on Indium Phosphide and Related Materials* (2009), pp. 120–123. Copyright 2009, IEEE.

Since Gossard’s work with Rodwell on high-speed electronics, regrowth has been explored as a method for improved III-V on Si heteroepitaxy and embedded dielectric photonic structures. While Gossard is not always directly cited in these papers, it speaks to his foresight and ingenuity that he was able to see the potential device applications before the technique became widespread. For example, Liu *et al.* later utilized a similar nonselective regrowth technique to grow DHBT structures compatible with Si CMOS.⁷ By growing a GaAs buffer on Ge and a graded InAlAs buffer, antiphase domains and threading dislocations can be reduced for InGaAs DHBTs grown on CMOS-compatible silicon substrates. However, this resulted in polycrystalline deposition on the unexposed portions of the wafer, which must then be dry etched similarly to Gossard and Bowers’ method to recover the surface. Nishimoto *et al.* were able to avoid the challenges of polycrystalline deposition from nonselective regrowth by overgrowing air holes rather than dielectric features.⁶ After etching holes into a GaAs substrate, regrowth resulted in the coalescence of the crystal above the etched holes leaving teardrop-shaped embedded air gaps in the layer structure. By carefully tuning the diameter and pitch of these air gaps, Nishimoto *et al.* were able to create a buried photonic crystal structure for use as the backside reflector in a surface emitting laser. Ironside *et al.* later achieved selective regrowth and planar coalescence in MBE regrowth by utilizing a group-III cyclic growth technique similar to Wistey’s method in the Gossard group.⁸ While Wistey and Gossard initially used MEE, which cycles both the group-III and group-V shutters, Ironside used periodic supply epitaxy (PSE), a technique similar to MME developed by Allegretti and Nishinaga¹⁷ that leaves a constant group-V overpressure while cycling only the group-III sources. However, in contrast to the low As flux MME, PSE uses a high As flux to encourage faceting. When performed at a substrate temperature of 630 °C, the diffusion and desorption of adatoms on the dielectric surface are enhanced leading to selective area growth by MBE. After the growth fronts started to coalesce above the

dielectric features, continuous growth was used to planarize the growth surface. Quantum wells grown above the buried dielectric features show photoluminescence comparable to a non-regrowth control, further indicating that MBE regrowth is suitable for device applications. By combining Wistey and Gossard’s cyclic growth for smooth, controlled faceting with coalescence seen in papers such as Nishimoto’s, MBE regrowth has proven itself to be a capable method for future device applications (Fig. 3).

III. DIGITAL ALLOY GROWTH

One subtle, yet far-reaching impact of Gossard’s work is his contribution to graded digital alloy heterostructure design and crystal growth. Gossard was one of the earliest adopters of what has been termed the digital alloy growth method. He recognized its importance for demonstrating fundamental features of low-dimensional materials science. Crucially, he understood the potential of arbitrary alloy grading capabilities afforded by digital growth, such as accurate and precise parabolic grading of AlGaAs/GaAs heterointerfaces. For brevity, we consider some of his key contributions to early digital alloy growth and how he used the method to advance III-V telecommunication emission devices. We also highlight how Gossard-inspired digital alloy growth advanced our research, leading to the development of the first low-noise III-V alloy family for short to midwave-IR avalanche photodiodes (APDs).

Graded-heterostructure semiconductor engineering was proposed by Kroemer in the late 1950s.¹⁸ Such structures were designed to produce quasioelectric fields that could be modulated by tuning the composition of semiconductor materials across a heterointerface. As highlighted by Kroemer in his Nobel lecture:¹⁹ the impact of quasioelectric fields produced by bandgap engineering between disparate materials “... present[s] a new degree of freedom for the device designer to enable him to obtain effects that are basically impossible to obtain using only ‘real’

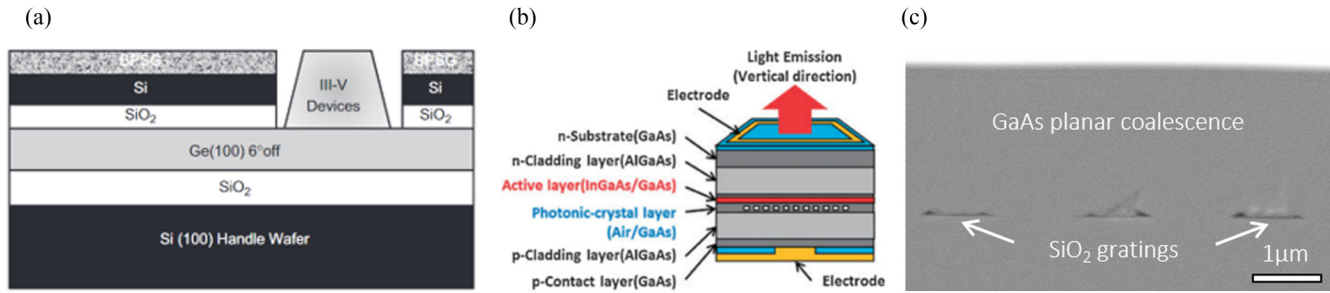


FIG. 3. (a) Diagram of nonselective selective regrowth for III-V devices integrated with CMOS. Reprinted with permission from Liu *et al.*, *J. Cryst. Growth* **311**, 1979 (2009). Copyright 2009, Elsevier. (b) Diagram of a photonic crystal cavity surface emitting laser that uses MBE regrowth to create a backside air hole photonic crystal. Reprinted with permission from Nishimoto *et al.*, *Appl. Phys. Express* **7**, 092703 (2014). Copyright 2014, The Japan Society of Applied Physics. (c) SiO₂ gratings embedded in GaAs using MBE regrowth. Reprinted with permission from Ironside *et al.*, *Cryst. Growth Des.* **19**, 3085 (2019). Copyright 2019, American Chemical Society.

electric fields.” Capasso later expanded on Kroemer’s original quasifield theory as so-called “bandgap engineering”²⁰ and used it to produce a series of intriguing graded-gap structures for use as high-speed transistors, resonators, and photodetectors.^{20–23}

Early realizations of graded-heterostructures were a nontrivial task. A crystal grower required fine control over their reactor’s elemental sources. Conventional MBE growth technique used to produce a graded heterointerfaces was essentially “analog” alloy growth, where a source oven temperature or valve was adjusted to control the molecular beam flux, which resulted in a modulated alloy molar fraction. For example, early analog growth experiments focused on the Al_xGa_{1-x}As/GaAs system, where the aluminum cell temperature was adjusted to modulate *x* and produce graded Al_xGa_{1-x}As layers. Analog alloy growth of graded-bandgap structures is tricky for several reasons. It relies on adjusting cell temperature, which is susceptible to thermal transients and cell ramp rates, leading to complications associated with undesired and potentially unstable growth rate change. The finite time required to adjust cell temperature set the limit for how accurately and precisely a graded layer could be grown. Also, cell flux versus temperature profiles had to be sufficiently large to account for the range of desired compositions. Early analog growth was further limited by early cell hardware controls, which limited graded-layer growth repeatability.²⁴ In addition to growth timing limitations, analog growth is also difficult to perform because analog alloys often have stringent growth requirements, namely, a limited growth temperature window, group-V flux requirements to stabilize the growing surface, and—in the presence of a thermodynamic miscibility gap²⁵—the potential for phase segregation.

An alternative approach is “digital” alloy growth. Originally termed as “pulsed” beam MBE by Kawabe *et al.* in the early 1980s,^{26,27} digital alloy growth involves an alternate deposition of layers to form short-period superlattices in the mono-/few-layer thickness range, where each period can be intentionally grown with different compositions. The duty cycle of the cell shutters is varied in a controlled manner such that a grower can produce structures with potential profiles of an almost arbitrary shape.²⁸ The period of digital alloy superlattices is much smaller than the de Broglie wavelengths of the carriers, which is typically several

tens of nanometers in semiconductors. As a result, digitally grown material behaves like a variable gap ordered alloy and the carrier “sees” the average alloy profile of the period.²⁰ Figure 4(a) gives a comparison of digital versus analog graded AlGaAs growth.

Digital alloy growth circumvents many of the challenges of graded analog alloy growth listed above.³⁰ Namely, digital growth eliminates the frequent change in the cell temperatures and the associated long flux stabilization times to produce graded compositions required by analog growth, leading to greater compositional control and reduced impurity incorporation. Another important benefit of the digital growth technique is that growers can use relatively high group-III fluxes and small group-V fluxes, resulting in faster growth rates and lower chamber pressure. Originally used to modulate group-III cell fluxes, digital growth was later extended to include group-V flux modulation³¹ and was used to demonstrate better composition repeatability than analog growth for mixed-V alloys.³² Digital growth can be used to more effectively strain-balance alloys, mitigating the deleterious effects of strain-induced surface roughening.³³ Digital alloy materials exhibit higher carrier mobilities due to reduced alloy scattering associated with the random arrangement of atoms in analog alloys³⁴ and excellent optical emission quality that is on par with or better than analog alloys.^{35–37} It is in many ways the short-period limit^{36,38–40} of superlattices.⁴¹ However, the term digital alloy has (informally) taken on a more general meaning beyond that of a short-period superlattice.

While at Bell Labs in the early 1980s, Gossard and co-workers used digitally grown Al_xGa_{1-x}As to realize the first parabolic quantum well structure,⁴² similar to that shown in Fig. 4. This seminal work exhibited controlled, even quantized level spacing long-assumed for parabolic potential structures. Gossard used the even level spacing of digital parabolic wells to clarify both the band offsets and effective mass electrons and holes in AlGaAs/GaAs quantum wells, which eliminated “forbidden” (or “non-diagonal”) optical transitions^{43,44} which plagued early quantum well design. For context, it is important to remember how important the AlGaAs/GaAs material system was for the nascent fields of III-V growth and devices – accurate heterojunction parameters used to design early quantum well structures were critical for the community’s eventual success.

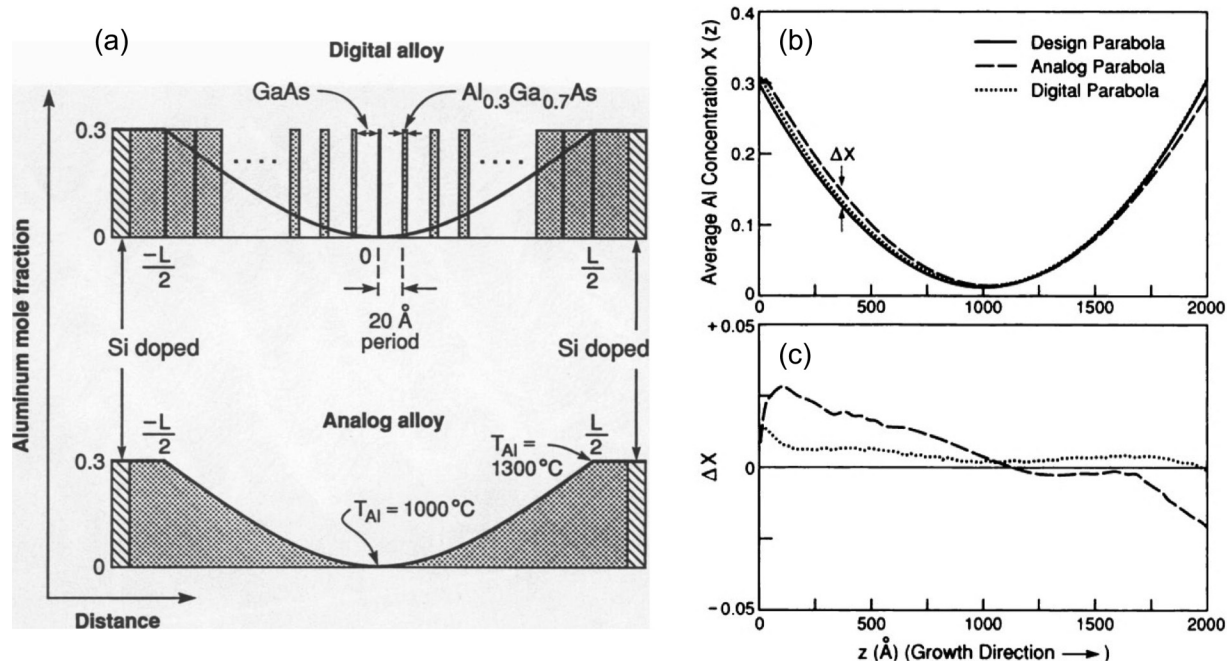


FIG. 4. Digital vs analog growth of a parabolic quantum well demonstrating $\text{Al}_x\text{Ga}_{1-x}\text{As}$ compositional grading. (a) Digital alloy growth by modulating the duty cycle of the Al shutter to produce an “average” x molar fraction per period. The same alloy profile produced using an analog alloy grade by tuning the Al cell temperature leading to modulated Al flux. Reprinted with permission from Sundaram *et al.*, *Science* **254**, 1326 (1991). Copyright 1991, AAAS. (b) Example of digital (dotted line) and analog growth (dashed line) compared to a target parabolic quantum well profile (solid line). Reproduced with permission from Sundaram *et al.*, *J. Vac. Sci. Technol. B* **9**, 1524 (1991). Copyright 1991, American Vacuum Society. (c) Compositional Al error between digital and analog growth, showing digital growth better produces the desired well profile, especially in the regions near the edge of the quantum well, where composition changes rapidly. Reprinted with permission from Sundaram *et al.*, *Science* **254**, 1326 (1991). Copyright 1991, AAAS.

Armed with a reliable method to produce a parabolic grade,³⁰ Gossard expanded on his earlier work with Dingle *et al.*⁴⁵ by using the digital alloy technique to modulation dope graded heterostructures.^{46,47} Like earlier modulation doping studies of square quantum wells, the spatial separation of ionized impurities from the free-carrier gas formed in the well mitigates impurity scattering leading to high mobility structures.⁴⁸ However, unlike square wells, a nearly flat band edge results from charge redistribution of donated electrons that fall into the wide parabolic wells, which results in a nearly uniform free-carrier gas that takes up a sufficiently large spatial region that multiple subbands of the well were occupied, termed a three-dimensional electron (3DEG),⁴⁹ like that shown in Fig. 5. Gossard demonstrated electron gases with mobilities $>2.5 \times 10^5 \text{ cm}^2/\text{Vs}$ using this method.^{50,51} Further work by Gossard used digitally graded parabolic structures for nonlinear optical terahertz intraband resonances⁵² and superlattice parabolic wells for coupled, high-mobility electron gases.^{53,54}

Arguably his greatest and most practical contribution to digital alloy growth was by implementing the technique to improve vertical cavity surface emitting lasers (VCSELs). While we consider a few specific examples of digital alloy growth, Gossard’s contributions to VCSELs are reviewed in more detail of this special issue by Coldren.¹²⁵ Historically, VCSELs relied on a more-or-less brute-

force approach, which used massive doping at the abrupt hetero-interfaces to reduce the distributed Bragg reflector (DBR) mirror series resistance; unfortunately, the exceedingly high doping required increased the optical losses of the mirrors caused by free-carrier absorption. In collaboration with Coldren, Gossard utilized the digital alloy growth method to technique to parabolically grade across the DBR mirror multilayers, which lead to flattening of the valence band that induces low-voltage hole transport without the need for extreme doping levels.⁵⁵ An example of this change is shown in Fig. 6(a). As a consequence, the mirror conductivity substantially increases without significant free-carrier optical losses. Additionally, higher compositions of aluminum could be used due to doping limitations in high aluminum-containing alloys, which produced greater index contrast in the DBR mirrors. The combination of these compounding, positive changes led to lower operating powers, higher efficiencies, and increased device speed.

Further work by Coldren incorporated digital alloy active regions (DAARs) to VCSEL structures, such as $\text{InGaAs}/\text{AlGaInAs}$ shown in Fig. 6(c), terming them submonolayer superlattices (SMSs).^{56,57} SMSs were viewed as an extension of early DA work, which typically utilized binary/binary or ternary/ternary in whole monolayer period thicknesses ($\sim 2\text{--}5 \text{ ML}$). The move to SMSs was

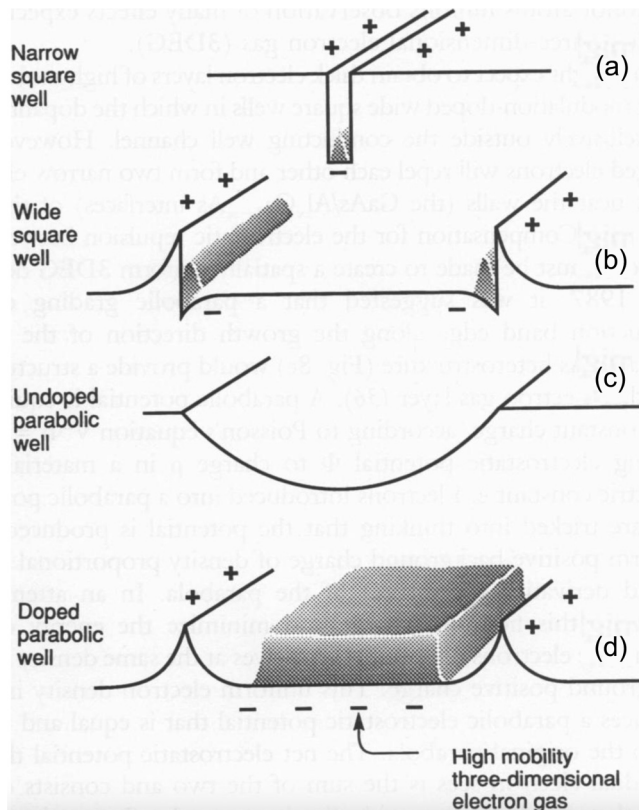


FIG. 5. 3DEG using a modulation-doped parabolic well. (a) Modulation doped (MD) narrow square quantum well, with ionized donor atoms (+) and electrons at the bottom of the well (-). (b) MD wide square quantum well, where the redistribution of charge produces a high-mobility free-carrier 2DEG. (c) Undoped wide parabolic well. (d) MD wide parabolic well. Electrons from the donors fall into the well, which screens the parabolic potential, leading to a large and nearly uniform 3DEG that occupies multiple subbands at the bottom of the flat region of the well. The separation of ionized impurities from the electron gas reduces ionized impurity scattering, which produces mobilities $>2.5 \times 10^5$ cm²/V s. Reprinted with permission from Sundaram *et al.*, *Science* **254**, 1326 (1991). Copyright 1991, AAAS.

required to maintain sufficiently thin QW active regions for the target emission wavelength and most active regions were grown on strained host lattices, making thick DA growth more difficult. With Coldren, Gossard extended their early VCSEL work into a cascaded or multiactive region (MAR) VCSEL, like that shown in Fig. 6(b), where the electrons that recombined in a DAAR could be “recycled” and injected as the minority carrier into the another DAAR stage. This was largely possible because of strain balancing afforded by the digital alloy method, which reduced the overall strain of the device and permitted the growth of such a thick structure.⁵⁸ From his early parabolic well demonstration to later VCSEL design enhancements, Gossard standardized digital alloy growth for use as both heterointerface grading and thick, bulklike regions.

The use of digital alloy grading also proved critical in improving the electrical characteristics and manufacturability of HBT

grown by MBE. With the transition from liquid phase epitaxy to MBE growth of AlGaAs/GaAs HBTs, the more abrupt heterointerfaces that MBE produces increased the turn-on voltage of the base-emitter junction. Analog compositional grading with MBE was shown to reduce this parasitic;⁵⁹ shortly thereafter, Gossard and co-workers showed that parabolic digital grading of the emitter could also solve this issue, but with the advantages in complexity and reproducibility noted earlier.⁶⁰

This approach became even more important with the rise of InP-based HBTs. Around 1990, InP/InGaAs/InP (emitter/base/collector) and InAlAs/InGaAs/InP DHBTs began to replace single heterojunction InP/InGaAs/InGaAs and InAlAs/InGaAs/InGaAs HBTs due to the increased breakdown voltage from the larger collector bandgap. This necessitated compositional grading to address both the emitter-base and base-collector junctions. MOCVD-grown InP/InGaAs/InP DHBTs used a “step-graded” InGaAs/InGaAsP/InP base-collector grade, with one or two InGaAsP layers. Some early MBE InP/InGaAs/InP DHBTs used an InGaAs base and an (InGaAs/InP) composite collector, with the thickness of the InGaAs layer in the collector chosen to yield an InGaAs/InP conduction-band barrier at an energy below that of the base conduction band. Unfortunately, this still resulted in an energy barrier at low collector voltages; moreover, the breakdown voltage was compromised by the narrow-bandgap InGaAs layer in the collector. A breakthrough came with the introduction of InAlAs/InP digital grading⁶¹ which—reproducibly and controllably—surmounted these limitations in MBE-grown DHBTs. This has become routine with the widespread use of the more easily grown InGaAs/InAlAs digital alloys to grade the emitter-base and base-collector junctions;⁶² moreover, these capabilities proved instrumental in enabling MBE to become the dominant technology for commercial HBT production.

One more recent impact of Gossard’s digital alloy legacy is the pursuit of low-noise III-V optical detectors. APDs are moderately reverse-biased junction detectors that rely on impact ionization as an internal gain mechanism. The high-field conditions produced from the applied field lead to faster carrier transit times, thus faster devices. Additionally, the presence of an internal gain mechanism can lead to excellent detector sensitivity to small input signals.⁶³ Bulk III-V binaries, like InSb, and ternaries, like InGaAs, were used to develop shortwave-IR (1–3 μm) and midwave-IR (3–5 μm) detectors but suffered from large impact ionization gain variation referred to as “excess noise” or “gain noise.” Si- and HgCdTe-based detectors have reigned supreme in the short and midwave-IR wavelength ranges in the recent years. However, their relatively large, indirect bandgaps (Si)⁶⁴ or manufacturing limitations (HgCdTe)⁶⁵ have prevented the development of a single material system that spans the short and midwave regimes, which takes advantages of the size, weight, and performance benefits of a solid-state platform. Progress has been made using bulk III-V for detectors, such as with high-quality InAs APDs,^{66,67} but a low-noise III-V 1–5 μm APD alternative to Si and HgCdTe has remained elusive.

Around the time Gossard worked with Awschalom in the early 2000s to reduce phase segregation in magnetic digital alloys, such as MnGaAs,^{68–70} Vaughn *et al.* adopted the digital alloy approach to tackle the same phase segregation problem observed in Al_xIn_{1-x}As_ySb_{1-y} alloys lattice-matched to GaSb for type-I midwave-IR lasers.⁷¹ In the early 2010s, we considered

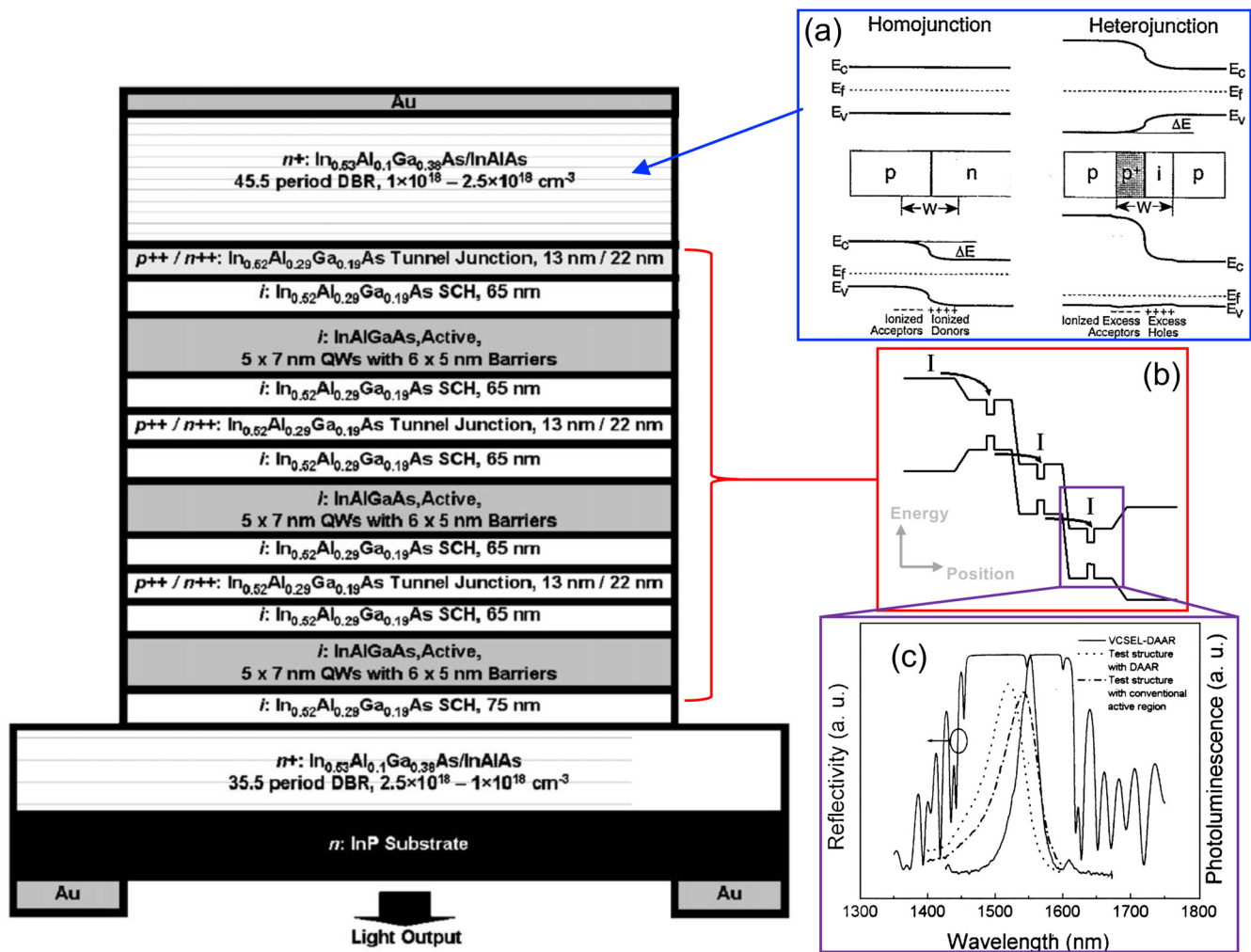


FIG. 6. Few Gossard-inspired digital alloy contributions to VCSEL design. (a) DBR utilizing a graded heterojunction instead of traditional homojunctions. Reproduced with permission from Peters *et al.*, *Appl. Phys. Lett.* **63**, 3411 (1993). Copyright 1993, AIP Publishing LLC. (b) MAR that incorporates [Reprinted with permission from Reddy *et al.*, *IEEE Photon. Technol. Lett.* **15**, 891 (2003). Copyright 2003, IEEE]. (c) Digital alloy active regions [Reprinted with permission from Wang *et al.*, *J. Cryst. Growth* **277**, 13 (2005)]. Copyright 2005, Elsevier]. (Left) A stack diagram of a digital alloy based VCSEL. Reprinted with permission from Wang *et al.*, *J. Cryst. Growth* **277**, 13 (2005). Copyright 2005, Elsevier.

using digital alloy AlInAsSb with Joe Campbell at the University of Virginia for tunable bandgap shortwave-IR detectors. We quickly discovered that it was a material system that was easy to manufacture over a large compositional range with a widely tunable direct bandgap ($\sim 0.25\text{--}1.25\text{ eV}$),⁷² and—as a happy accident—found AlInAsSb to be the first low-noise III-V alloy family.^{73,74}

Further investigations later revealed the digital alloy growth technique was—at least in part—responsible for these low-noise properties.⁷⁵ In the years following, digital alloy growth of AlInAsSb enabled a series of low-noise, tunable bandgap 1–5 μm cutoff APDs in Fig. 4, including conventional p-i-n; photodiodes,^{76–79} separate charge, absorber, and multiplier (SACM) APDs,^{80–83} and the first

true realization of Capasso’s “staircase APD”—the solid-state implementation of the photomultiplier tube (Fig. 7).^{84,85}

IV. METAL:SEMICONDUCTOR NANOCOMPOSITES

Metal:semiconductor nanocomposites are a fantastic example of the divergent thinking and critical understanding that Art Gossard has brought to research, connecting fundamental physical insights with myriad and seemingly disparate device applications. The kernel of the idea that became nanostructured materials can be traced through much of Gossard’s early work. Zero-dimensional quantum-confined structures were initially considered from a top-down

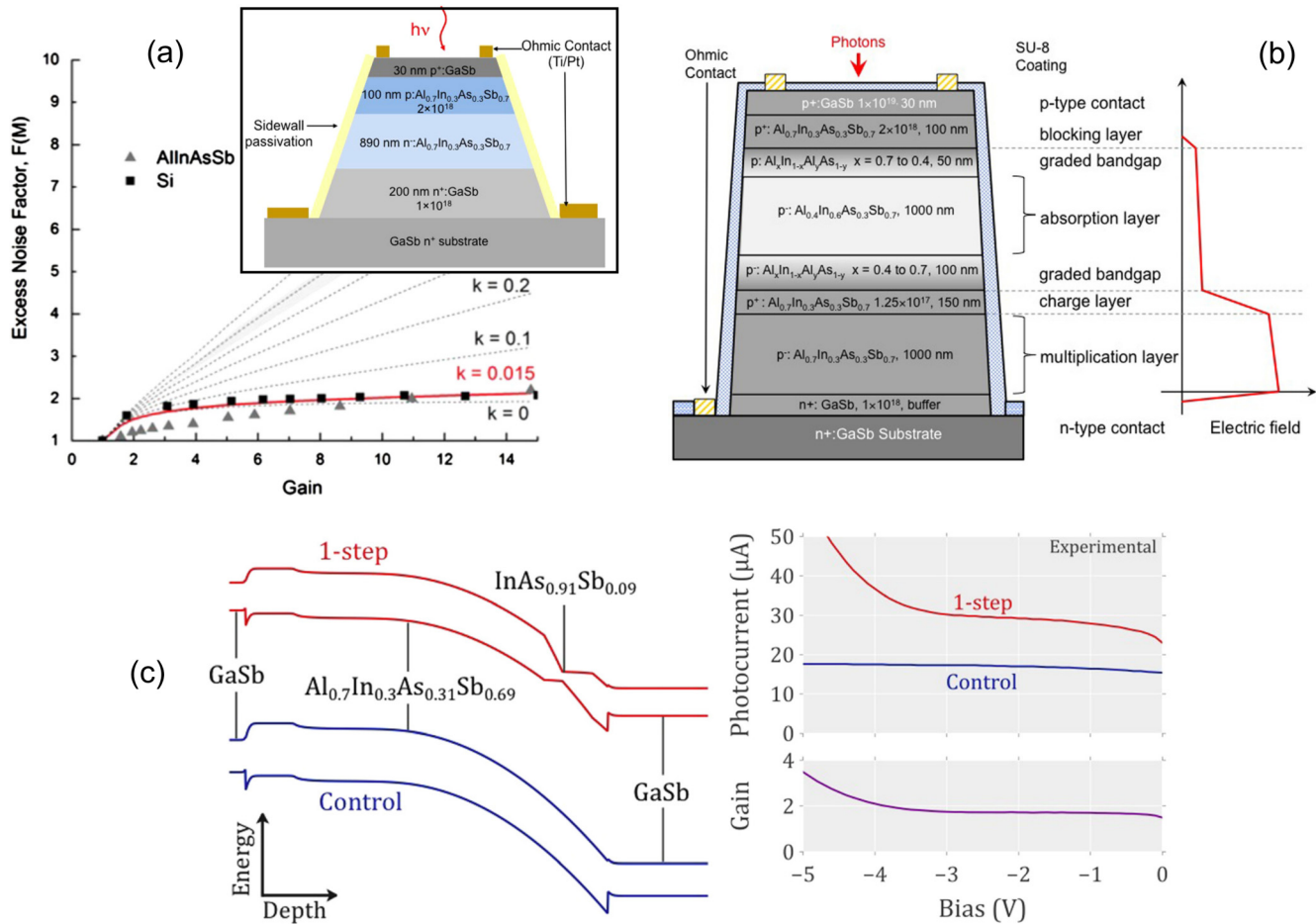


FIG. 7. Examples of low-noise III-V APDs using digital alloy AllnAsSb lattice matched to GaSb. (a) Conventional p-i-n photodiode APD showing low-noise ($k \sim 0$). Reproduced with permission from Woodson *et al.*, Appl. Phys. Lett. **108**, 081102 (2016). Copyright 2016, AIP Publishing LLC. (b) SACM APD, which takes advantage of a low-field, narrow-bandgap absorber and a high-field, wide-bandgap avalanche multiplication region. Reproduced with permission from Ren *et al.*, Appl. Phys. Lett. **108**, 191108 (2016). Copyright 2016, AIP Publishing LLC. (c) Staircase APD with a step gain of $\sim 2\times$, which was the first clear demonstration of Capasso's (Ref. 84) long-sought solid-state analog of the photomultiplier tube. Reproduced with permission from Ren *et al.*, Appl. Phys. Lett. **108**, 081101 (2016). Copyright 2016, AIP Publishing LLC.

approach as a natural extension of his work on superlattices and quantum wells in the GaAs/AlGaAs system,⁸⁶ preceding bottom-up approaches such as self-assembled InAs quantum dots that are revolutionizing diverse fields from quantum information processing⁸⁷ to silicon photonics.⁸⁸ His pre-MBE work involved the nuclear-magnetic-resonance characterization of many species—often single-moment measurements on rare-earth compounds.^{89–91} Prior work on the epitaxial integration of rare-earths as dopants by Sethi and co-workers⁹² and as layered films by Palmström and co-workers⁹³ laid the groundwork for Gossard's research into the morphological control and utility of rare-earth nanocomposites. III-V materials typically do not wet to complete rare-earth-group-V (RE-V) films, whereas adjacent nanocomposites leave exposed III-V between them, allowing for subsequent III-V films to grow coherently.^{93,94} Here, we will consider primarily Gossard's work with ErAs

nanocomposites in III-As host media, though similar results have often been obtained in other systems,⁹⁵ including ErSb in III-Sb materials.^{96–99} The success of ErAs nanocomposites in the device applications described herein have elevated broader RE-V from a materials pursuit to a significant tool for high-performance device design. Consequently, other rare-earth species have also been explored for more targeted device applications; for a thorough overview of rare-earth nanocomposites and films in III-V epitaxy, please see Ref. 95.

The initial efforts of Gossard and collaborators into RE-V nanocomposites led to the profound increase in tunability and thermal robustness of ErAs:GaAs terahertz devices over then-dominant LT-GaAs.¹⁰⁰ The ultrafast recombination of LT-GaAs requires careful annealing postgrowth; this fundamental temperature sensitivity leads to thermally induced degradation after prolonged

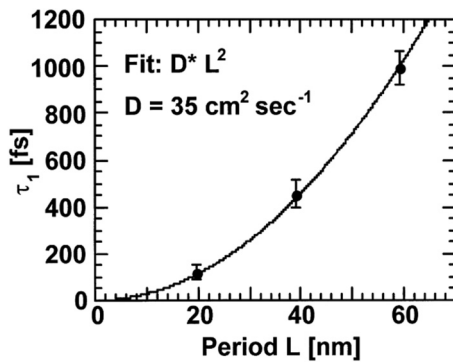


FIG. 8. Diffusion-limited lifetimes for ErAs:GaAs superlattices. Reproduced with permission from Kadow *et al.*, *Appl. Phys. Lett.* **75**, 3548 (1999). Copyright 1999, AIP Publishing LLC.

use. ErAs:GaAs nanocomposites are, however, thermodynamically stable, yielding more consistent long-term performance. While Gupta *et al.* had previously shown carrier lifetimes as low as 1 ps for GaAs with homogeneous Er doping,⁹² Gossard and collaborators were able to reduce the carrier lifetime to 120 fs by deliberately growing ErAs nanocomposites embedded in the GaAs matrix, leveraging earlier work on the epitaxial growth of ErAs nanocomposites by Palmström and co-workers.⁹³ Critically, they showed that the carrier lifetime could be directly controlled with the separation between consecutive nanocomposite layers and that the carrier lifetime was purely limited by the diffusion time, rather than by any relaxation process within the nanocomposites themselves (Fig. 8). Later works demonstrated photoconductors based on ErAs:GaAs, eventually outperforming LT-GaAs and radiation-damaged silicon-on-sapphire in both amplitude

and bandwidth^{101–103} and leading to a new class of ultrafast reconfigurable photonic devices.¹⁰⁴

Attempts to use ErAs:InGaAs for terahertz generation and sensing at 1550 nm, leveraging the maturity and availability of telecom optical components compared to those near 850 nm, were then a natural progression. However, early efforts provided an additional challenge: ErAs nanocomposites produced strongly n-type InGaAs, violating the essential resistivity requirements for photoconductors.¹⁰⁵ The dependence of electrical conduction on the nanocomposite size showed the critical role that ErAs nanocomposites have in tuning the Fermi energy. Delta doping the ErAs nanocomposites proved an effective means to increase the resistivity of ErAs:InGaAs films, and device results presented the first photoconductors pumped at 1550 nm.¹⁰⁶ More recently, photoconductors for emission have embedded ErAs nanocomposites in thin, p-type InAlAs surrounded by InGaAs absorbers, further increasing dark resistivity and showing complete spectroscopy systems with state-of-the-art performance.^{107,108}

The highly n-type nature of uncompensated ErAs:InGaAs, while a challenge for THz photoconductors, proved essential for thin-film thermoelectrics.¹⁰⁹ Here, the strong n-type doping without significant carrier mobility degradation coupled to efficient mid- and long-wavelength phonon scattering from randomly distributed ErAs nanocomposites [Fig. 9(a)] acted as an effective means to achieve simultaneously high electrical conductivity and low thermal conductivity, thereby increasing thermoelectric power factors and Seebeck coefficients.¹¹⁰ The inclusion of digitally-grown (Sec. III) InAlGaAs layers provides a means to increase the Seebeck coefficient¹¹¹ and further creates a filter for high frequency phonons through superlattice effects [Fig. 9(c)]; this was initially noted by Gossard and collaborators in the context of GaAs/AlGaAs superlattices.¹¹²

High-resistivity ErAs:InGaAs was elusive because the Fermi energy of ErAs sits near the conduction-band minimum in InGaAs. Gossard and collaborators showed that the Fermi energy

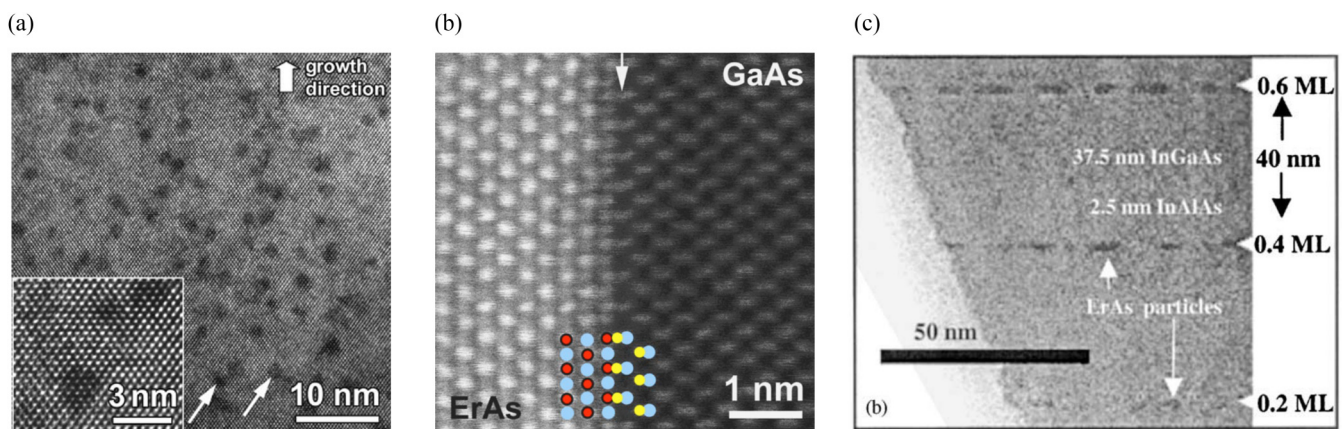


FIG. 9. (a) Randomly distributed ErAs nanocomposites in InGaAs. Reproduced with permission from Zide *et al.*, *Appl. Phys. Lett.* **87**, 2003 (2005). Copyright 2005, AIP Publishing LLC. (b) Complete ErAs films grown on GaAs. Reproduced with permission from Klenov *et al.*, *Appl. Phys. Lett.* **86**, 1 (2005). Copyright 2005, AIP Publishing LLC. (c) ErAs nanocomposites embedded in an InGaAs/InAlAs superlattice for high-performance THz photoconductors. Reprinted with permission from Hanson *et al.*, *Phys. E Low Dimens. Syst. Nanostruct.* **13**, 602 (2002). Copyright 2002, Elsevier.

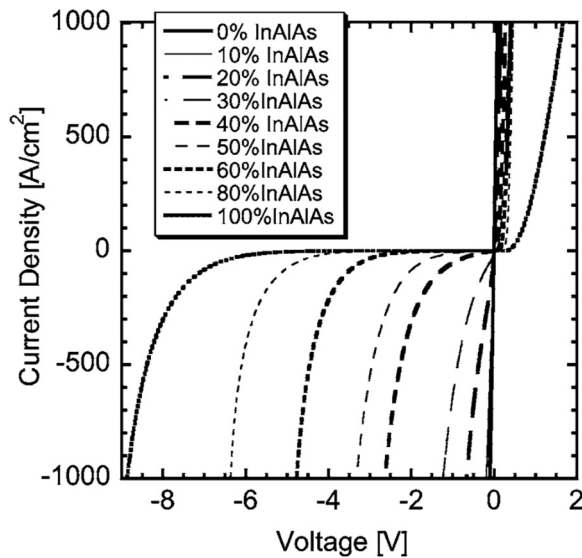


FIG. 10. IV characteristics from ErAs nanocomposite enhanced Schottky-barrier diodes. Reproduced with permission from Zimmerman *et al.*, *J. Vac. Sci. Technol. B* **23**, 1929 (2005). Copyright 2005, American Vacuum Society.

of semimetallic ErAs nanocomposites sat near the conduction-band minimum in InGaAs; the Fermi energy was also shown to be controllable through nanocomposite morphology and doping. RE-V nanocomposites then provided the ability to control the local Fermi energy, which proved paramount for semiconductor-metal contacts and tunnel junctions. The use of quaternary host media provided additional freedom to tune the conduction-band minimum and valence-band maximum with respect to the Fermi energy. This was beautifully demonstrated with a continuous ErAs film on InAlGaAs with varying compositions to produce an all-epitaxial, tunable Schottky diode system with a near-perfect correlation between the Schottky barrier height and conduction band offsets, shown in Fig. 10.¹¹⁵ Furthermore, the surface metal-semiconductor interface remained epitaxially clean, which was shown to produce Schottky barrier THz detectors with significantly decreased noise.¹¹⁶ In the low-Al limit, the Schottky barrier height is minimized, allowing for high tunneling probability; this was leveraged to create low-resistance contacts suitable for transistors with THz operating frequencies.¹¹⁷ Partial overgrowth and increasing ErAs deposition was shown to create textured interfaces through nanocomposite stacking, further increasing the tunability of ErAs/III-As from morphology alone.¹¹⁸

ErAs nanocomposites placed at the interface of a p-n junction provide an exceedingly high number of electronic states at the ErAs Fermi energy. As in the low-Al limit above, this leads to high tunneling probability and therefore efficient electron-hole generation via band-to-band tunneling.¹¹⁹ RE-enhanced tunnel junctions supply orders of magnitude more current than heavily-doped homojunctions, with subsequent work showing that the tunneling current could be enhanced still further via the growth conditions.¹²⁰ Gossard and co-workers demonstrated the first application of these

“nanoparticle-enhanced” tunnel junctions to practical devices, particularly high-efficiency, multijunction solar cells¹²¹ and cascaded nipnip photomixers.^{122,123} Noteworthy is that these tunnel junctions found commercial application in multijunction solar cells with record-breaking solar conversion efficiencies.¹²⁴

V. CONCLUSION

We reviewed a small subset of Art’s historic and ongoing contributions to modern electronic and photonic devices, set in the context of three illustrative case-studies that have been particularly influential to—and enabling for—our own research efforts. They speak to Art’s unique abilities to *both* invent new materials/synthesis approaches to solve device problems, *as well as* identify new device applications for novel materials. Art’s unique ability to not only perform the fundamental materials science necessary to develop new materials, but also to successfully apply novel materials research to concretely advance device performance, puts him in rarefied air as one of the most influential, impactful, and collaborative material scientists of this era.

In Sec. II, we reviewed Art’s contributions to epitaxial regrowth with MBE. In the near-term, this enables new device capabilities such as reduced parasitics in RF/power transistors and selective-area integration of III-V devices with Si CMOS (with both MBE and MOCVD). Looking further to the future, as these capabilities continue to develop, one can imagine the monolithic integration of traditionally heterogeneous materials becoming commonplace in devices. Section III focused on digital alloy growth, which Art developed into a method for realizing reliable compositional grading for the first time with MBE, as well as used for the first time to grow high-performance VCSELs. His work on digital alloy GaMnAs growth set the stage for the digital alloy method to emerge as a means to entirely avoid phase segregation challenges, opening up new alloy compositions to device researchers. The digital alloy method continues to develop as the ultimate generalization of the superlattice. In the future, it promises to offer a fundamentally new materials design paradigm for controlling and manipulating traditionally “fundamental” materials properties, with control of impact ionization processes in APDs likely serving as only the first such example. Section IV reviewed Art’s pioneering work integrating RE-V nanostructures with crystalline III-V semiconductors to yield a new class of designer metal:semiconductor nanocomposites; he showed could be used to advance the performance of devices ranging from THz sources and detectors, to multijunction solar cells, and even thermoelectrics.

Looking forward into the future, Art’s work points us toward the eventual convergence of these seemingly disparate topics. The seamless integration of atomically-designed semiconductors, with dielectrics and metals, into a single epitaxial stack would open a rich new device design space for device physics to explore. Such a capability, should it eventually emerge, will undoubtedly lead to radically new electronic/photonic device architectures and functionality over the coming years.

ACKNOWLEDGMENTS

M.J.W.R. and S.R.B. are honored to have had the opportunity to work closely with Art; we have benefited tremendously from these interactions, both directly from his insights and innovations, as

well as indirectly from learning how he chooses unique tacts to approach challenging new problems. A.J.M., A.M.S., and S.D.M. thank Art for enabling their research over the years through his many contributions to materials science and MBE growth. We gratefully acknowledge Joshua Zide for many useful discussions regarding the choice of topics and applications discussed in this article, as well as the opportunity to participate in this Special Issue.

DATA AVAILABILITY

Data sharing is not applicable to this article as no new data were created or analyzed in this study.

REFERENCES

- ¹J. J. Hsieh and C. C. Shen, *Appl. Phys. Lett.* **30**, 429 (1977).
- ²M. Hirao, A. Doi, S. Tsuji, M. Nakamura, and K. Aiki, *J. Appl. Phys.* **51**, 4539 (1980).
- ³K. Utaka, S. Akiba, K. Sakai, and Y. Matsushima, *Electron. Lett.* **17**, 961 (1981).
- ⁴I. Mito, M. Kitamura, K. Kobayashi, S. Murata, M. Seki, Y. Odagiri, H. Nishimoto, M. Yamaguchi, and K. Kobayashi, *J. Lightwave Technol.* **1**, 195 (1983).
- ⁵R. S. Tucker and I. P. Kaminow, *J. Lightwave Technol.* **2**, 385 (1984).
- ⁶M. Nishimoto, K. Ishizaki, K. Maekawa, Y. Liang, K. Kitamura, and S. Noda, *Appl. Phys. Express* **7**, 092703 (2014).
- ⁷W. K. Liu *et al.*, *J. Cryst. Growth* **311**, 1979 (2009).
- ⁸D. J. Ironside, A. M. Skipper, T. A. Leonard, M. Radulaski, T. Sarmiento, P. Dhingra, M. L. Lee, J. Vučković, and S. R. Bank, *Cryst. Growth Des.* **19**, 3085 (2019).
- ⁹Y. Wei, D. W. Scott, Y. Dong, A. C. Gossard, and M. J. Rodwell, *IEEE Electron Device Lett.* **25**, 232 (2004).
- ¹⁰D. W. Scott, Y. Wei, Y. Dong, A. C. Gossard, and M. J. Rodwell, *IEEE Electron Device Lett.* **25**, 360 (2004).
- ¹¹G. J. Burek, M. A. Wistey, U. Singiseti, A. Nelson, B. J. Thibeault, S. R. Bank, M. J. Rodwell, and A. C. Gossard, *J. Cryst. Growth* **311**, 1984 (2009).
- ¹²U. Singiseti *et al.*, *Phys. Status Solidi C* **6**, 1394 (2009).
- ¹³M. A. Wistey, U. Singiseti, A. K. Baraskar, G. J. Burek, A. C. Gossard, and M. J. W. Rodwell, "Improved migration-enhanced epitaxy for self-aligned InGaAs devices," in *Proceedings of EMC* (University Park, PA, 2009); available at https://web.ece.ucsb.edu/Faculty/rodwell/publications_and_presentations/publications/2009_6_june_wistey EMC_digest.pdf. EMC 2009 was in University Park, PA.
- ¹⁴U. Singiseti *et al.*, *IEEE Electron Device Lett.* **30**, 1128 (2009).
- ¹⁵M. A. Wistey, A. K. Baraskar, U. Singiseti, G. J. Burek, B. Shin, E. Kim, P. C. McIntyre, A. C. Gossard, and M. J. W. Rodwell, *J. Vac. Sci. Technol. B* **33**, 011208 (2015).
- ¹⁶U. Singiseti *et al.*, in *IEEE International Conference on Indium Phosphide & Related Materials* (IEEE, Newport Beach, CA, 2009), pp. 120–123.
- ¹⁷F. E. Allegretti and T. Nishinaga, *J. Cryst. Growth* **156**, 1 (1995).
- ¹⁸H. Kroemer, *RCA Rev.* **18**, 332 (1957).
- ¹⁹H. Kroemer, *Int. J. Mod. Phys. B* **16**, 677 (2002).
- ²⁰F. Capasso, *Ann. Rev. Mater. Sci.* **16**, 263 (1986).
- ²¹F. Capasso, *Semicond. Semimet.* **24**, 319 (1987).
- ²²F. Capasso, *Science* **235**, 172 (1987).
- ²³F. Capasso, H. M. Cox, A. L. Hutchinson, N. A. Olsson, and S. G. Hummel, *Appl. Phys. Lett.* **45**, 1193 (1984).
- ²⁴J. P. Harbison, L. D. Peterson, and J. Levkoff, *J. Cryst. Growth* **81**, 34 (1987).
- ²⁵K. Onabe, *Jpn. J. Appl. Phys.* **21**, L323 (1982).
- ²⁶M. Kawabe, N. Matsuura, K. Toda, and H. Inuzuka, *Jpn. J. Appl. Phys.* **21**, 439 (1982).
- ²⁷M. Kawabe, M. Kondo, N. Matsuura, and K. Yamamoto, *Jpn. J. Appl. Phys.* **22**, L64 (1983).
- ²⁸W. Geißelbrecht, U. Pfeiffer, A. Thränhardt, U. Klütz, A. C. Gossard, and G. H. Döhler, *J. Cryst. Growth* **201**, 163 (1999).
- ²⁹M. Sundaram *et al.*, *Science* **254**, 1326 (1991).
- ³⁰M. Sundaram, A. Wixforth, R. S. Geels, A. C. Gossard, and J. H. English, *J. Vac. Sci. Technol. B* **9**, 1524 (1991).
- ³¹Y. H. Zhang, *J. Cryst. Growth* **150**, 838 (1995).
- ³²E. Hall, H. Kroemer, and L. A. Coldren, *J. Cryst. Growth* **203**, 447 (1999).
- ³³A. G. Norman *et al.*, *Appl. Phys. Lett.* **73**, 1844 (1998).
- ³⁴J. P. André, A. Deswarte, E. Lugagne-delpont, P. Voisin, and P. Ruterana, *J. Electron. Mater.* **23**, 141 (1994).
- ³⁵S. Jourba, M. Gendry, O. Marty, M. Pitaval, and G. Hollinger, *Appl. Phys. Lett.* **75**, 220 (1999).
- ³⁶V. A. Kulbachinskii, R. A. Lunin, V. A. Rogozin, V. G. Mokerov, Y. V. Fedorov, Y. V. Khabarov, and A. De Visser, *Semicond. Sci. Technol.* **17**, 947 (2002).
- ³⁷S. M. Wang, T. G. Andersson, W. Q. Chen, U. Södervall, and J. Thordson, *J. Cryst. Growth* **135**, 455 (1994).
- ³⁸T. Nakayama and H. Kamimura, *J. Phys. Soc. Jpn.* **54**, 4726 (1985).
- ³⁹M. Recio, J. L. Castaño, and F. Briones, *Jpn. J. Appl. Phys.* **27**, 1204 (1988).
- ⁴⁰Y. Taniyasu and M. Kasu, *Appl. Phys. Lett.* **99**, 7 (2011).
- ⁴¹L. Esaki and R. Tsu, *IBM J. Res. Dev.* **14**, 61 (1970).
- ⁴²R. C. Miller, A. C. Gossard, D. A. Kleinman, and O. Munteanu, *Phys. Rev. B* **29**, 3740 (1984).
- ⁴³R. C. Miller, D. A. Kleinman, and A. C. Gossard, *Phys. Rev. B* **29**, 7085 (1984).
- ⁴⁴R. C. Miller, A. C. Gossard, and D. A. Kleinman, *Phys. Rev. B* **32**, 5443 (1985).
- ⁴⁵R. Dingle, H. L. Störmer, A. C. Gossard, and W. Wiegmann, *Appl. Phys. Lett.* **33**, 665 (1978).
- ⁴⁶M. Sundaram, A. C. Gossard, and P. O. Holtz, *J. Appl. Phys.* **69**, 2370 (1991).
- ⁴⁷M. Sundaram and A. C. Gossard, *J. Appl. Phys.* **73**, 251 (1993).
- ⁴⁸W. Walukiewicz, P. F. Hopkins, M. Sundaram, and A. C. Gossard, *Phys. Rev. B* **44**, 10909 (1991).
- ⁴⁹B. I. Halperin, *Jpn. J. Appl. Phys.* **26**, 1913 (1987).
- ⁵⁰E. G. Gwinn, R. M. Westervelt, P. F. Hopkins, A. J. Rimberg, M. Sundaram, and A. C. Gossard, *Phys. Rev. B* **39**, 6260 (1989).
- ⁵¹A. Wixforth, M. Sundaram, K. Ensslin, J. H. English, and A. C. Gossard, *Appl. Phys. Lett.* **56**, 454 (1990).
- ⁵²W. W. Bewley, C. L. Felix, J. J. Plombon, M. S. Sherwin, M. Sundaram, P. F. Hopkins, and A. C. Gossard, *Phys. Rev. B* **48**, 2376 (1993).
- ⁵³J. H. Baskey, A. J. Rimberg, S. Yang, R. M. Westervelt, P. F. Hopkins, and A. C. Gossard, *Appl. Phys. Lett.* **61**, 1573 (1992).
- ⁵⁴M. Sundaram, A. Wixforth, P. F. Hopkins, and A. C. Gossard, *J. Appl. Phys.* **72**, 1460 (1992).
- ⁵⁵M. G. Peters, B. J. Thibeault, D. B. Young, J. W. Scott, F. H. Peters, A. C. Gossard, and L. A. Coldren, *Appl. Phys. Lett.* **63**, 3411 (1993).
- ⁵⁶M. H. Reddy, A. Huntington, D. Buell, R. Koda, E. Hall, and L. A. Coldren, *Appl. Phys. Lett.* **80**, 3509 (2002).
- ⁵⁷M. H. Reddy, D. A. Buell, D. Feezell, T. Asano, R. Koda, A. S. Huntington, and L. A. Coldren, *IEEE Photonics Technol. Lett.* **15**, 891 (2003).
- ⁵⁸C. S. Wang, R. Koda, A. S. Huntington, A. C. Gossard, and L. A. Coldren, *J. Cryst. Growth* **277**, 13 (2005).
- ⁵⁹P. M. Abbeck, D. L. Miller, R. A. Milano, J. S. Harris, G. R. Kaelin, and R. Zucca, "(Ga, Al)As/GaAs bipolar transistors for digital integrated circuits," in *1981 International Electron Devices Meeting* (IEEE, Washington DC, 1981), pp. 629–632.
- ⁶⁰J. R. Hayes, F. Capasso, R. J. Malik, A. C. Gossard, and W. Wiegmann, "Elimination of the emitter/collector offset voltage in heterojunction bipolar transistors," in *1983 International Electron Devices Meeting* (IEEE, Washington DC, 1983), pp. 686–689.
- ⁶¹R. C. Gee, C. L. Lin, C. W. Farley, C. W. Seabury, J. A. Higgins, P. D. Kirchner, J. M. Woodall, and P. M. Abbeck, *Electron. Lett.* **29**, 850 (1993).
- ⁶²W. Liu, *Handbook of III-V Heterojunction Bipolar Transistors* (Wiley, New York, 1998).
- ⁶³B. L. Kasper and J. C. Campbell, *J. Lightwave Technol.* **5**, 1351 (1987).

- ⁶⁴J. C. Campbell, "Advances in photodetectors," in *Optical Fiber Telecommunications V A: Components and Subsystems* (Elsevier Inc., New York, 2008), pp. 221–268.
- ⁶⁵A. Rogalski, P. Martyniuk, and M. Kopytko, *Appl. Phys. Rev.* **4**, 031304 (2017).
- ⁶⁶P. J. Ker, A. R. Marshall, A. B. Krysa, J. P. David, and C. H. Tan, "InAs electron avalanche photodiodes with 580 GHz gain-bandwidth product," in *Technical Digest – 2012 17th Opto-Electronics and Communications Conference, OECC 2012* (IEEE, Busan, South Korea, 2012), pp. 220–221.
- ⁶⁷W. Sun, S. J. Maddox, S. R. Bank, and J. C. Campbell, *Device Res. Conf. Dig.* **49**, 47 (2014).
- ⁶⁸R. K. Kawakami, E. Johnston-Halperin, L. F. Chen, M. Hanson, N. Guébels, J. S. Speck, A. C. Gossard, and A. A. Awschalom, *Appl. Phys. Lett.* **77**, 2379 (2000).
- ⁶⁹T. C. Kreutz, G. Zanelatto, E. G. Gwinn, and A. C. Gossard, *Appl. Phys. Lett.* **81**, 4766 (2003).
- ⁷⁰T. C. Kreutz, W. D. Allen, G. Zanelatto, E. G. Gwinn, and A. C. Gossard, *Phys. Rev. B* **70**, 1 (2004).
- ⁷¹L. G. Vaughn, L. R. Dawson, E. A. Pease, L. F. Lester, H. Xu, Y. Jiang, and A. L. Gray, *Phys. Simul. Optoelectron. Devices XIII* **5722**, 307 (2005).
- ⁷²S. J. Maddox, S. D. March, and S. R. Bank, *Cryst. Growth Des.* **16**, 3582 (2016).
- ⁷³M. E. Woodson, M. Ren, S. J. Maddox, Y. Chen, S. R. Bank, and J. C. Campbell, *Appl. Phys. Lett.* **108**, 081102 (2016).
- ⁷⁴S. R. Bank, J. C. Campbell, S. J. Maddox, M. Ren, A. K. Rockwell, M. E. Woodson, and S. D. March, *IEEE J. Sel. Top. Quantum Electron.* **24**, 3800407 (2018).
- ⁷⁵A. K. Rockwell *et al.*, *Appl. Phys. Lett.* **113**, 102106 (2018).
- ⁷⁶M. Ren, S. J. Maddox, M. E. Woodson, Y. Chen, S. R. Bank, and J. C. Campbell, *J. Lightwave Technol.* **35**, 2380 (2017).
- ⁷⁷A.-K. Rockwell, Y. Yuan, A. H. Jones, S. D. March, S. R. Bank, and J. C. Campbell, *IEEE Photonics Technol. Lett.* **30**, 1048 (2018).
- ⁷⁸Y. Yuan, J. Zheng, A. K. Rockwell, S. D. March, S. R. Bank, and J. C. Campbell, *IEEE Photonics Technol. Lett.* **31**, 315 (2019).
- ⁷⁹A. H. Jones, A.-K. Rockwell, S. D. March, Y. Yuan, S. R. Bank, and J. C. Campbell, *IEEE Photonics J.* **31**, 1948 (2019).
- ⁸⁰M. Ren, S. J. Maddox, M. E. Woodson, Y. Chen, S. R. Bank, and J. C. Campbell, *Appl. Phys. Lett.* **108**, 191108 (2016).
- ⁸¹Y. Lyu *et al.*, *J. Cryst. Growth* **482**, 70 (2018).
- ⁸²X. Yi, S. Xie, B. Liang, L. W. Lim, J. S. Cheong, M. C. Debnath, D. L. Huffaker, C. H. Tan, and J. P. David, *Nat. Photonics* **13**, 683 (2019).
- ⁸³A. H. Jones, S. D. March, S. R. Bank, and J. C. Campbell, *Nat. Photonics* **14**, 559 (2020).
- ⁸⁴F. Capasso and G. F. Williams, *IEEE Trans. Nucl. Sci.* **30**, 381 (1983).
- ⁸⁵M. Ren, S. Maddox, Y. Chen, M. Woodson, J. C. Campbell, and S. Bank, *Appl. Phys. Lett.* **108**, 081101 (2016).
- ⁸⁶J. Cibert, P. M. Petroff, G. J. Dolan, S. J. Pearton, A. C. Gossard, and J. H. English, *Appl. Phys. Lett.* **49**, 1275 (1986).
- ⁸⁷A. Imamoglu, D. D. Awschalom, G. Burkard, D. P. DiVincenzo, D. Loss, M. Sherwin, and A. Small, *Phys. Rev. Lett.* **83**, 4204 (1999).
- ⁸⁸J. C. Norman *et al.*, *IEEE J. Quantum Electron.* **55**, 1 (2019).
- ⁸⁹A. C. Gossard and V. Jaccarino, *Proc. Phys. Soc.* **80**, 877 (1962).
- ⁹⁰A. C. Gossard, T. Y. Kometani, and J. H. Wernick, *J. Appl. Phys.* **39**, 849 (1968).
- ⁹¹E. Bucher, K. Andres, F. J. Di Salvo, J. P. Maita, A. C. Gossard, A. S. Cooper, and G. W. Hull, *Phys. Rev. B* **11**, 500 (1975).
- ⁹²S. Gupta, S. Sethi, and P. K. Bhattacharya, *Appl. Phys. Lett.* **62**, 1128 (1993).
- ⁹³S. J. Allen, N. Tabatabaie, C. J. Palmström, G. W. Hull, T. Sands, F. DeRosa, H. L. Gilchrist, and K. C. Garrison, *Phys. Rev. Lett.* **62**, 2309 (1989).
- ⁹⁴D. R. Schmidt, A. G. Petukhov, M. Foygel, J. P. Ibbetson, and S. J. Allen, *Phys. Rev. Lett.* **82**, 823 (1999).
- ⁹⁵C. C. Bomberger, M. R. Lewis, L. R. Vanderhoef, M. F. Doty, and J. M. O. Zide, *J. Vac. Sci. Technol. B* **35**, 030801 (2017).
- ⁹⁶J. K. Kawasaki, B. D. Schultz, H. Lu, A. C. Gossard, and C. J. Palmström, *Nano Lett.* **13**, 2895 (2013).
- ⁹⁷M. P. Hanson, A. C. Gossard, and E. R. Brown, *Appl. Phys. Lett.* **89**, 111908 (2006).
- ⁹⁸J. P. Feser, D. Xu, H. Lu, Y. Zhao, A. Shakouri, A. C. Gossard, and A. Majumdar, *Appl. Phys. Lett.* **103**, 103102 (2013).
- ⁹⁹H. Lu, P. G. Burke, A. C. Gossard, G. Zeng, A. T. Ramu, J. H. Bahk, and J. E. Bowers, *Adv. Mater.* **23**, 2377 (2011).
- ¹⁰⁰C. Kadow, S. B. Fleischer, J. P. Ibbetson, J. E. Bowers, A. C. Gossard, J. W. Dong, and C. J. Palmström, *Appl. Phys. Lett.* **75**, 3548 (1999).
- ¹⁰¹C. Kadow, A. W. Jackson, A. C. Gossard, S. Matsuura, and G. A. Blake, *Appl. Phys. Lett.* **76**, 3510 (2000).
- ¹⁰²J. E. Bjarnason, T. L. Chan, A. W. Lee, E. R. Brown, D. C. Driscoll, M. Hanson, A. C. Gossard, and R. E. Muller, *Appl. Phys. Lett.* **85**, 3983 (2004).
- ¹⁰³J. F. O'Hara, J. M. Zide, A. C. Gossard, A. J. Taylor, and R. D. Averitt, *Appl. Phys. Lett.* **88**, 1 (2006).
- ¹⁰⁴H.-T. Chen, W. J. Padilla, J. M. O. Zide, S. R. Bank, A. C. Gossard, A. J. Taylor, and R. D. Averitt, *Opt. Lett.* **32**, 1620 (2007).
- ¹⁰⁵D. C. Driscoll, M. Hanson, C. Kadow, and A. C. Gossard, *Appl. Phys. Lett.* **78**, 1703 (2001).
- ¹⁰⁶M. Sukhotin, E. R. Brown, A. C. Gossard, D. Driscoll, M. Hanson, P. Maker, and R. Muller, *Appl. Phys. Lett.* **82**, 3116 (2003).
- ¹⁰⁷U. Nandi, J. C. Norman, A. C. Gossard, H. Lu, and S. Preu, *J. Infrared Millim. Terahertz Waves* **39**, 340 (2018).
- ¹⁰⁸U. Nandi, F. R. Faridi, A. D. Olvera, J. Norman, H. Lu, A. C. Gossard, and S. Preu, "High dynamic range THz systems using ErAs:In(Al)GaAs photoconductors," in *IMWS-AMP 2019–2019 IEEE MTT-S International Microwave Workshop Series on Advanced Materials and Processes for RF and THz Applications* (IEEE, Bochum, Germany, 2019), p. 115.
- ¹⁰⁹J. M. Zide, D. O. Klenov, S. Stemmer, A. C. Gossard, G. Zeng, J. E. Bowers, D. Vashaee, and A. Shakouri, *Appl. Phys. Lett.* **87**, 112102 (2005).
- ¹¹⁰W. Kim, J. Zide, A. Gossard, D. Klenov, S. Stemmer, A. Shakouri, and A. Majumdar, *Phys. Rev. Lett.* **96**, 1 (2006).
- ¹¹¹J. M. Zide, D. Vashaee, Z. X. Bian, G. Zeng, J. E. Bowers, A. Shakouri, and A. C. Gossard, *Phys. Rev. B* **74**, 1 (2006).
- ¹¹²V. Narayanamurti, H. L. Störmer, M. A. Chin, A. C. Gossard, and W. Wiegmann, *Phys. Rev. Lett.* **43**, 2012 (1979).
- ¹¹³D. O. Klenov *et al.*, *Appl. Phys. Lett.* **86**(24), 1 (2005).
- ¹¹⁴M. Hanson *et al.*, *Physica E* **13**, 602 (2002).
- ¹¹⁵J. D. Zimmerman, E. R. Brown, and A. C. Gossard, *J. Vac. Sci. Technol. B* **23**, 1929 (2005).
- ¹¹⁶A. C. Young, J. D. Zimmerman, E. R. Brown, and A. C. Gossard, *Appl. Phys. Lett.* **88**, 073518 (2006).
- ¹¹⁷U. Singiseti, J. D. Zimmerman, M. A. Wistey, J. Cagnon, B. J. Thibeault, M. J. Rodwell, A. C. Gossard, S. Stemmer, and S. R. Bank, *Appl. Phys. Lett.* **94**, 10 (2009).
- ¹¹⁸J. D. Zimmerman, A. C. Gossard, A. C. Young, M. P. Miller, and E. R. Brown, *J. Vac. Sci. Technol. B* **24**, 1483 (2006).
- ¹¹⁹P. Pohl *et al.*, *Appl. Phys. Lett.* **83**, 4035 (2003).
- ¹²⁰H. P. Nair, A. M. Crook, and S. R. Bank, *Appl. Phys. Lett.* **96**, 222104 (2010).
- ¹²¹J. M. Zide, A. Kleiman-Shwarsstein, N. C. Strandwitz, J. D. Zimmerman, T. Steenblock-Smith, A. C. Gossard, A. Forman, A. Ivanovskaya, and G. D. Stucky, *Appl. Phys. Lett.* **88**, 162103 (2006).
- ¹²²M. Eckardt *et al.*, *Physica E* **17**, 629 (2003).
- ¹²³F. Renner *et al.*, *Phys. Status Solidi A* **202**, 965 (2005).
- ¹²⁴M. W. Wiemer, H. B. Yuen, V. A. Sabnis, M. J. Sheldon, and I. Fushman, "Functional integration of dilute nitrides into high efficiency III-V solar cells," U.S. patent 2010/0319764 A1 (December 23, 2010).
- ¹²⁵L. A. Coldren, *J. Vac. Sci. Technol. A* **39**, 010801 (2021).